Role of neutron transfer in the enhancement of sub-barrier fusion excitation functions of various systems using an energy-dependent Woods-Saxon potential

Manjeet Singh Gautam*
Department of Physics, Kurukshetra University, Kurukshetra-136119, India
(Received 20 March 2014; revised manuscript received 26 April 2014; published 28 August 2014)

The focus of the present article is to address the effects of the role of a neutron transfer channel in the enhancement of sub-barrier fusion excitation function data of various heavy-ion systems by using an energy-dependent Woods-Saxon potential (EDWSP) model in conjunction with the one-dimensional Wong's formula and the coupled-channel model by using the code CCFULL. The effects of coupling to neutron transfer channels are found to have dominance over the coupling to low-lying surface vibrational states, such as the 2^+ and 3^- vibrational states. Furthermore, the influence of inelastic surface excitations and the effects of six neutron transfer channels with positive ground state Q values are mocked up by the EDWSP model.

DOI: 10.1103/PhysRevC.90.024620 PACS number(s): 25.60.Pj, 21.60.Ev, 24.10.Eq

I. INTRODUCTION

The development of the availability of radioactive beams and particle accelerator technologies enable researchers to explore the many possibilities of the nuclear interactions between colliding nuclei. Heavy-ion fusion reactions at sub-barrier energies have received more attention during the past few decades because these reactions contain valuable information with regard to the nuclear structure of reacting nuclei and their nuclear interactions. The fusion of two nuclei, wherein the two colliding nuclei come close together with a sufficient kinetic energy that results in the formation of a compound nucleus either by overcoming or by a quantum-mechanical tunneling through the fusion barrier is one of the most interesting and puzzling process. The simplest theoretical way to understand the fusion of the two nuclei is the barrier penetration model, wherein the reactants are assumed to penetrate through their fusion barrier due to its wave nature and form a composite nucleus. Fusion reactions, which occur at below barrier energies, show anomalously large enhancement in the fusion cross section over the predictions of the one-dimensional barrier penetration model [1–5]. For many projectile-target combinations, this enhancement can be understood in terms of the various physical effects that arise due to the internal degrees of freedom of the participating nuclei. Indeed, the coupling of the relative motion of the colliding nuclei to various intrinsic degrees of freedom, such as low-lying surface vibrational states, rotational states, neck dynamics, neutron transfer reactions, etc., enhances the sub-barrier fusion cross section by several orders of magnitude in comparison to the one-dimensional barrier penetration model calculations. All these effects, which occur in the surface region of the nuclear potential or tail region of the Coulomb barrier, are responsible for the fluctuation in the surface diffuseness of the reactants and lead to the requirement of the larger value of the diffuseness parameter of the static Woods-Saxon potential. This reflects the inconsistency of the static Woods-Saxon potential, which has been used in various coupled-channel calculations, for simultaneously exploring the elastic-scattering and heavy-ion fusion reactions [1–20]. The coupled-channel models predict that the order of magnitude of the enhancement of the sub-barrier fusion cross section increases with the product $Z_P Z_T$, but also displays large isotopic variations [1–6]. However, in certain cases, a suppression of the fusion cross section in comparison to the coupled-channel calculations in the deep sub-barrier energy region has also been observed [21–27], which is found to have a link with the diffuseness anomaly [7–11]. Therefore, the suppression or enhancement of the sub-barrier fusion cross section is a debatable issue.

Three factors, such as static deformations, the surface vibrations of colliding nuclei, and the neutron transfer channels are identified as major factors which are responsible for anomalously large enhancement of the sub-barrier fusion cross section. The coupled-channel models accurately describe the fusion enhancement due to static deformations and inelastic surface vibrations of colliding nuclei [1–18,28–39]. However, the fusion enehancement due to neutron transfer channels has not been fully understood because multineutron transfer feels no Couomb barrier and hence starts the transfer between the reactants at larger internuclear separations. The coupling to neutron transfer channels will effectively reduce the fusion barrier and hence will enhance the sub-barrier fusion excitation function data [40–42]. Theoretical and experimental studies suggest that the neutron tranfer channels (particularly the neutron pickup channels with ground-state positive Q values) are partially or fully responsible for the dramatic energy dependence of the fusion cross section at sub-barrier energies.

In the nuclear reaction studies, the shape of the nucleus-nucleus potential, which consists of the Coulomb repulsive interaction, a centrifugal term, and the attractive short-range nuclear potential, is one of the most essential ingredient. The Coulomb and centrifugal terms are well understood, whereas there are large ambiguities in the optimum form of the nuclear potential. The success of any theoretical approach depends upon the choice of the nuclear potential which contains some free parameters, and many attempts have been made to extract the information about the form of the nuclear potential from the experimental data so that the dramatic behavior of the sub-barrier fusion cross section can be

*gautammanjeet@gmail.com

fully accounted. In literature, various parametrizations of the nuclear potential have been used for explaining the variety of different phenomena in connection with heavy-ion reactions [14–20,43–54]. In the case of the most commonly adopted three parametric Woods-Saxon potential as used in the code CCFULL [55], the diffuseness parameter defines the slope of the nuclear potential in the tail region of the Coulomb barrier. This indicates that a value of the diffuseness parameter is one of the most sensitive parameter in heavy-ion fusion reactions. Since, up to first order, the coupling strength is proportional to the deformation length and the first-order derivative of the nuclear potential with respect to r (radial separation), the diffuseness parameter directly influences the coupling strengths [56]. A value of diffuseness parameter $a = 0.65$ fm has been deduced from the elastic-scattering data, and it is interesting to note that a wide range ($a = 0.75$ to $a = 1.5$ fm) of values of the diffuseness parameter is required to explore the sub-barrier fusion data. The cause of such a diffuseness anomaly is still far from being clearly understood [1–27,56].

In heavy-ion fusion reactions, the introducing of energy dependence in the nucleus-nucleus real potential in such a way that it becomes more attractive at energies in the vicinity of the Coulomb barrier is another underlying physical effect that can produce a similar kind of channel coupling effect as obtained in coupled-channel calculations [14–20]. The nucleus-nucleus potential is a fundamental characteristic of heavy-ion fusion reactions. When such an energy-dependent nucleus-nucleus potential is used in the phenomenological one-dimensional barrier penetration model, it will lower the effective fusion barrier and will predict a larger sub-barrier fusion cross section in comparison to that of the energy-independent one-dimensional barrier penetration model as evident from the present paper [the energy-dependent Woods-Saxon potential (EDWSP) model] [14–18]. It is reasonable to consider the energy dependence in the nucleus-nucleus potential because it has also been pointed out in the double-folding potential, wherein it arises due to the energy dependence of the underlying nucleon-nucleon interactions and from the nonlocal quantum effects [14,20]. An energy-dependent parametrization of the Woods-Saxon potential, proposed in an earlier paper, was successfully used to explain the description of the sub-barrier fusion cross sections of various systems [14–18]. The present paper is a systematic study of the fusion excitation function data for various heavy-ion systems by using two different models: the energy-dependent Woods-Saxon potential in conjunction with the one-dimensional Wong's formula [14–18,57] and the energy-independent Woods-Saxon potential in the coupled-channel model by using the code CCFULL [55], wherein the coupling to multiphonon vibrational states can be properly handled.

Since the energy dependence of the sub-barrier fusion cross section is quite sensitive to the nuclear structure of colliding nuclei for highlighting the specific features of the sub-barrier fusion process, it is necessary to consider the most suitable projectile-target combinations. The fusion of the $^{40,48}_{20}\mathrm{Ca} + {}^{90,96}_{40}\mathrm{Zr}$ and $^{40}_{20}\mathrm{Ca} + {}^{94}_{40}\mathrm{Zr}$ systems has been well studied, and probably these are the most suitable candidates to isolate the importance of the neutron transfer channels. The coupled-channel analysis predicts that the fusion of the $^{40}_{20}\mathrm{Ca} + {}^{90}_{40}\mathrm{Zr}$ and $^{48}_{20}\mathrm{Ca} + {}^{90,96}_{40}\mathrm{Zr}$ systems is dominated by inelastic surface excitations, whereas in the fusion of the $^{40}_{20}\mathrm{Ca} + {}^{94,96}_{40}\mathrm{Zr}$ systems, there is a rich interplay of neutron transfer channels and inelastic surface excitations [6,56,58–66]. Very recently, a systematic study of the fusion of the $^{40,48}_{20}\mathrm{Ca} + {}^{90,96}_{40}\mathrm{Zr}$ systems [64,65] by using the energy-independent Woods-Saxon potential, the M3Y + repulsive, and the double-folding potentials within the framework of the coupled-channel model reveals that the influence of neutron transfer channels plays a decisive role in explaining the fusion of the $^{40}_{20}\mathrm{Ca} + {}^{96}_{40}\mathrm{Zr}$ system, whereas the fusion of the other three Ca + Zr combinations can be well accounted for by including low-lying surface vibrations of the colliding nuclei. Furthermore, the authors predicted that a good explanation of the fusion dynamics of the $^{40}_{20}\mathrm{Ca} + {}^{96}_{40}\mathrm{Zr}$ system may be achieved either with an adjusted Woods-Saxon potential or with a pure M3Y potential along with the coupling to the neutron transfer channel for this system. Jiang *et al.* [66] have reported a similar conclusion by analyzing the fusion dynamics of Ca + Zr combinations by using the one-dimensional Wong's formula. Furthermore, the authors found that the shallower slope of the fusion excitation function data result in a larger barrier curvature for their corresponding fusion barrier and ultimately leads to the fusion enhancement in the sub-barrier energy region. Thus, the larger fusion enhancement for the $^{40}_{20}\mathrm{Ca} + {}^{96}_{40}\mathrm{Zr}$ system in comparison to the other three Ca + Zr systems can be correlated with the possibility of the neutron transfer channels which should be necessarily included in the coupled-channel model so that an accurate description of the fusion mechanism can be achieved.

The present article deals with the fusion of the $^{40,48}_{20}\mathrm{Ca} + {}^{90,96}_{40}\mathrm{Zr}$ and $^{40}_{20}\mathrm{Ca} + {}^{94}_{40}\mathrm{Zr}$ systems within the context of the EDWSP model and the coupled-channel model. The anomaly in the fusion of these systems lies in the relative importance of the multiphonon vibrational states and the neutron transfer channels, which has been not fully recovered. It will be evident from the present paper that the EDWSP model, which is much more simpler than the various coupled-channel models [1–5,34], accurately explains the fusion dynamics of the various heavy-ion systems, and a wide range of diffuseness parameters is needed to reproduce the fusion excitation function data. A brief description of the method of calculation is given in Sec. II. The results are discussed in detail in Sec. III, whereas the conclusions drawn are presented in Sec. IV.

II. THEORETICAL FORMALISM

A. The one-dimensional Wong's formula

The partial-wave expansion for the reaction cross section leads to the following expression for the fusion cross section:

$$\sigma_F = \frac{\pi}{k^2} \sum_{\ell=0}^{\infty} (2\ell + 1) T_\ell^F . \tag{1}$$

To obtain a simple expression for the fusion probability (T_ℓ^F), one can use the Hill and Wheeler approximation, wherein the effective potential near the barrier radius is approximated by a

parabola [16,17,67],

$$V_\ell(r) \cong V_\ell - \frac{\mu\omega_\ell^2}{2}(r - R_\ell)^2, \tag{2}$$

with

$$V_\ell = V_B + \frac{\ell(\ell+1)\hbar^2}{2\mu r^2}, \tag{3}$$

so that the transmission probability can be written as

$$T_\ell^{\rm HW} = \frac{1}{1 + \exp\left[\frac{2\pi}{\hbar\omega_\ell}(V_\ell - E)\right]}. \tag{4}$$

The above Hill-Wheeler expression is exact for a parabolic barrier but is an approximate expression for the potential barrier in heavy-ion collisions. For fusion reactions, Wong further simplifies the Hill-Wheeler approximation by using the following assumptions for barrier position, barrier curvature, and barrier height [1–5,16,17,57,68,69]:

$$R_\ell = R_{\ell=0} = R_B, \tag{5}$$

$$\omega_\ell = \omega_{\ell=0} = \omega, \tag{6}$$

$$V_\ell = V_B + \frac{\hbar^2}{2\mu R_B^2}\left[\ell + \frac{1}{2}\right]^2. \tag{7}$$

Since Wong assumes that infinite numbers of partial waves contribute to the fusion process to change the summation over ℓ into an integral over ℓ by combining Eqs. (4)–(7) with Eq. (1) and by solving the integral one can find the following final expression of Wong's formula, which can be used for evaluating the fusion cross section in all energy regions [1–5,34,55–57]:

$$\sigma_F = \frac{\hbar\omega R_B^2}{2E}\ell n\left[1 + \exp\left(\frac{2\pi}{\hbar\omega}(E - V_B)\right)\right]. \tag{8}$$

B. Coupled-channel model

In this section the details of the coupled-channel model, wherein the coupling of the relative motion with the intrinsic degrees of freedom of the colliding partners are entertained, are presented [3–5,15,55]. The set of coupled-channel equations can be written as

$$\left[\frac{-\hbar^2}{2\mu}\frac{d^2}{dr^2} + \frac{J(J+1)\hbar^2}{2\mu r^2} + V_N(r) + \frac{Z_P Z_T e^2}{r} + \varepsilon_n - E_{cm}\right] \times \psi_n(r) + \sum_m V_{nm}(r)\psi_m(r) = 0, \tag{9}$$

here, r is the radial coordinate for the relative motion between fusing nuclei. μ is defined as the reduced mass of the colliding nuclei. The quantities E_{cm} and ε_n represent the bombarding energy in the center of the mass frame and the excitation energy of the nth channel, respectively. V_{nm} is the matrix elements of the coupling Hamiltonian, which in the collective model consists of Coulomb and nuclear components.

For the coupled-channel calculations, one can use the code CCFULL [55], wherein the coupled-channel equations are solved numerically by imposing the two basic approximations. The first approximation is the no-Coriolis or rotating-frame approximation, which has been used to reduce the number of coupled-channel equations [15,39,43,70]. As the coupled-channel equations are solved by assuming that the centrifugal potential remains the same in all channels, it is also known as the isocentrifugal approximation. The second approximation is to use the in-going wave-boundary conditions (IWBCs). According to the IWBC there are only incoming waves at $r = r_{\rm min}$, the starting point of integration, which is taken as the minimum position of the Coulomb pocket inside the barrier, and there are only outgoing waves at infinity for all channels except the entrance channel ($n = 0$). In the code CCFULL [15,55], the energy-independent Woods-Saxon parametrization of the nuclear potential has been adopted

$$V_N(r) = \frac{-V_0}{\left[1 + \exp\left\{\frac{r - R_0}{a}\right\}\right]}, \tag{10}$$

with $R_0 = r_0(A_P^{1/3} + A_T^{1/3})$ where the quantities V_0 and a, respectively, are the strength and the diffuseness parameter. By including all the relevant channels, the fusion cross section can be written as

$$\sigma_F(E) = \sum_J \sigma_J(E) = \frac{\pi}{k_0^2}\sum_J (2J+1)P_J(E), \tag{11}$$

where $P_J(E)$ is the total transmission coefficient that corresponds to the angular momentum J. In the code CCFULL the rotational coupling with a pure rotor and a vibrational coupling in the harmonic limit are taken into account [55]. The operator in the nuclear coupling Hamiltonian for rotational and vibrational couplings is given by

$$\hat{O}_R = \beta_2 R_T Y_{20} + \beta_4 R_T Y_{40},$$

and

$$\hat{O}_V = \frac{\beta_\lambda}{\sqrt{4\pi}} R_T(a_{\lambda 0}^\dagger + a_{\lambda 0}), \tag{12}$$

respectively. Above R_T is parametrized as $r_{\rm coup}A^{1/3}$, β_λ are the deformation parameters, and $a_{\lambda 0}^\dagger(a_{\lambda 0})$ is the creation (annihilation) operator of the phonon of the vibrational mode of multipolarity λ. In general, the nuclear coupling matrix elements are evaluated as

$$V_{nm}^{(N)} = \langle n|V_N(r, \hat{O})|m\rangle - V_N^{(0)}\delta_{n,m}.$$

For the rotational couplings, the matrix elements of $\hat{O}_R$ between the $|n\rangle = |I0\rangle$ and the $|m\rangle = |I'0\rangle$ states of the rotational band and the matrix elements of the $\hat{O}_V$ between the n-phonon state $|n\rangle$ and the m-phonon state $|m\rangle$ are needed for the vibrational coupling, which are given by

$$\hat{O}_{R(I,I')} = \sqrt{\frac{5(2I+1)(2I'+1)}{4\pi}}\beta_2 R_T \begin{pmatrix} I & 2 & I' \\ 0 & 0 & 0 \end{pmatrix}^2 + \sqrt{\frac{9(2I+1)(2I'+1)}{4\pi}}\beta_4 R_T \begin{pmatrix} I & 4 & I' \\ 0 & 0 & 0 \end{pmatrix}^2, \tag{13}$$

and

$$\hat{O}_{V(nm)} = \frac{\beta_\lambda}{\sqrt{4\pi}} R_T(\delta_{n,m-1}\sqrt{m} + \delta_{n,m+1}\sqrt{n}), \tag{14}$$

respectively.

The Coulomb coupling matrix elements are computed by the linear coupling approximation and are given by

$$V^{(C)}_{R(I,I')} = \frac{3Z_P Z_T R_T^2}{5r^3}\sqrt{\frac{5(2I+1)(2I'+1)}{4\pi}}\left(\beta_2 + \frac{2}{7}\beta_2^2\sqrt{\frac{5}{\pi}}\right) \times \begin{pmatrix} I & 2 & I' \\ 0 & 0 & 0 \end{pmatrix}^2 + \frac{3Z_P Z_T R_T^4}{9r^5}\sqrt{\frac{9(2I+1)(2I'+1)}{4\pi}} \times \left(\beta_4 + \frac{9}{7}\beta_2^2\right)\begin{pmatrix} I & 4 & I' \\ 0 & 0 & 0 \end{pmatrix}^2, \quad (15)$$

and

$$V^{(C)}_{V(nm)} = \frac{\beta_\lambda}{\sqrt{4\pi}}\frac{3}{2\lambda+1}Z_P Z_T e^2 \frac{R_T^\lambda}{r^{\lambda+1}}(\sqrt{m}\delta_{n,m-1} + \sqrt{n}\delta_{n,m+1}) \quad (16)$$

for the rotational and vibrational couplings, respectively. The total coupling matrix elements are obtained by taking the sum of $V^{(N)}_{nm}$ and $V^{(C)}_{nm}$.

III. RESULTS AND DISCUSSION

The calculations have been performed for the fusion excitation functions of various heavy-ion systems by using the energy-dependent Woods-Saxon potential in conjunction with Wong's formula [1–5,16–18,57,68,69] and by using the coupled-channel code CCFULL [55]. In the present analysis, the inclusion of approximately 16 relevant channels in the coupled-channel calculations are sufficient to reproduce the fusion excitation function data for various projectile-target combinations. In the EDWSP model, the depth of the energy-dependent Woods-Saxon potential is defined as

$$V_0 = \left[A_P^{2/3} + A_T^{2/3} - (A_P + A_T)^{2/3}\right] \times \left[2.38 + 6.8(1 + I_P + I_T)\frac{A_P^{1/3}A_T^{1/3}}{\left(A_P^{1/3} + A_T^{1/3}\right)}\right]\text{MeV}, \quad (17)$$

where $I_P = (\frac{N_P - Z_P}{A_P})$ and $I_T = (\frac{N_T - Z_T}{A_T})$ are the isospin asymmetry of the projectile and the target nuclei, respectively. The energy dependence in the Woods-Saxon potential is employed through its diffuseness parameter, which is given by following expression:

$$a(E) = 0.85\left[1 + \frac{r_0}{13.75\left(A_P^{-(1/3)} + A_T^{-(1/3)}\right)\left[1 + \exp\left(\frac{\frac{E}{V_B} - 0.96}{0.03}\right)\right]}\right]\text{fm}. \quad (18)$$

The above energy-dependent Woods-Saxon potential simultaneously includes the effects of the surface energy as well as the isospin asymmetry of the colliding nuclei [14–18]. In the present paper, the sub-barrier fusion of the $^{40,48}_{20}$Ca + $^{90,96}_{40}$Zr and $^{40}_{20}$Ca + $^{94}_{40}$Zr systems has been discussed, and the values of the deformation parameters and the corresponding excitation energies of the low-lying 2^+ and 3^- vibrational states of all these nuclei are listed in Table I.

TABLE I. The deformation parameter (β_λ) and the energy (E_λ) of the quadrupole and octupole vibrational states of various nuclei.

Nucleus	β_2	E_2(MeV)	β_3	E_3(MeV)	Reference
$^{40}_{20}$Ca	0.12	3.904	0.43	3.737	[59]
$^{48}_{20}$Ca	0.11	3.832	0.23	4.507	[59]
$^{90}_{40}$Zr	0.09	2.186	0.22	2.748	[59]
$^{92}_{40}$Zr	0.10	0.934	0.17	2.340	[59]
$^{94}_{40}$Zr	0.09	0.919	0.20	2.058	[59]
$^{96}_{40}$Zr	0.08	1.751	0.27	1.897	[59]

The values of range, depth, and diffuseness of the EDWSP model calculations for various combinations of projectile and target nuclei are listed in Table II. In the present analysis, the range parameter (r_0) has been taken as a free parameter to vary the values of diffuseness of the nuclear potential by using Eq. (18), whereas the depth of the real part of the Woods-Saxon potential is obtained by using Eq. (17) [14–18]. The barrier height, barrier position, and barrier curvature of the fusing nuclei as required in the EDWSP model are taken from Refs. [6,16,56,59].

For all fusing systems, the range, depth, and diffuseness parameter of the static Woods-Saxon potential, which are required as input in the code CCFULL are listed in Table III. The fusion of projectile-target combinations which involves magic and doubly magic nuclei, such as the $^{40}_{20}$Ca + $^{90}_{40}$Zr and $^{48}_{20}$Ca + $^{90,96}_{40}$Zr systems, are of great interest because their analysis will lead to an unambiguous concrete conclusion with regard to the fusion dynamics and will shade light on the shape of the nucleus-nucleus potential. For both projectiles, 2^+ and 3^- vibrational states lie at high excitation energies, but their 2^+ states lie at almost the same excitation energy, which has comparable strength. Besides high excitation energy, the strength of the 3^- vibrational state of the lighter projectile $^{40}_{20}$Ca is much stronger as compared to that of the heavier projectile. Therefore, the inclusion of the 3^- vibrational state in the projectile $^{40}_{20}$Ca will be expected to produce more pronounced effects in the enhancement of the sub-barrier fusion cross section [6,59]. The comparison of deformation parameters and their corresponding excitation energies of the projectiles, which are listed in Table I, clearly indicate that the heavier calcium isotope $^{48}_{20}$Ca is more rigid than the lighter projectile $^{40}_{20}$Ca.

TABLE II. Range, depth, and diffuseness of the Woods-Saxon nuclear potential used in the present model calculations for various systems [14–18].

System	r_0 (fm)	V_0 (MeV)	$\frac{a^{\text{Present}}}{\text{Energy range}\left(\frac{\text{fm}}{\text{MeV}}\right)}$
$^{40}_{20}$Ca + $^{90}_{40}$Zr	1.120	104.20	$\frac{0.97-0.85}{85-120}$
$^{40}_{20}$Ca + $^{94}_{40}$Zr	1.123	109.05	$\frac{0.98-0.85}{80-120}$
$^{40}_{20}$Ca + $^{96}_{40}$Zr	1.123	111.33	$\frac{0.98-0.85}{80-120}$
$^{48}_{20}$Ca + $^{90}_{40}$Zr	1.085	130.51	$\frac{0.97-0.85}{85-120}$
$^{48}_{20}$Ca + $^{96}_{40}$Zr	1.085	139.03	$\frac{0.97-0.85}{85-120}$

TABLE III. Range, depth, and diffuseness of the static Woods-Saxon potential used in the coupled-channel calculations for various heavy-ion systems [6,56,59].

System	r_0 (fm)	V_0 (MeV)	a (fm)
$^{40}_{20}$Ca + $^{90}_{40}$Zr	1.090	120.00	75
$^{48}_{20}$Ca + $^{90}_{40}$Zr	1.112	113.90	68
$^{48}_{20}$Ca + $^{96}_{40}$Zr	1.050	127.80	85
$^{40}_{20}$Ca + $^{94}_{40}$Zr	1.050	116.20	90
$^{40}_{20}$Ca + $^{96}_{40}$Zr	1.050	120.00	90

In the fusion of the $^{40}_{20}$Ca + $^{90}_{40}$Zr system, both projectile and target are doubly magic nuclei and possess only low lying surface vibrational states as the dominant mode of couplings. In the coupled-channel analysis, the no-coupling calculation, wherein both colliding nuclei are considered inert, they are substantially underpredicted by the experimental data. Owing to significantly larger octupole deformation, which leads to the larger octupole coupling strength, the strong influence of coupling to this vibrational state is expected on the energy dependence of the sub-barrier fusion excitation function data. This mirrors the existence of a strong octupole vibrational state in the lighter projectile $^{40}_{20}$Ca. However, only coupling to the 3^- vibrational state of the projectile is unable to reproduce the experimental data, but it strongly enhances the sub-barrier fusion cross section in comparison to the coupling to one phonon 2^+ and 3^- vibrational states of the target and their mutual couplings. This suggests the necessity of coupling to higher phonon vibrational states of the target. Thus, the coupling to the double-phonon octupole vibrational states along with their mutual excitations, such as $(2^+)^2$, $(3^-)^2$, and $(2^+ \otimes 3^-)$ states in the target and single phonon 2^+ and 3^- vibrational states in the projectile reproduce the fusion data in a reasonable way as shown in Fig. 1.

The addition of more phonons in the target does not change the result, so there is no need to consider coupling to the higher phonon vibrational states, such as the three phonon, four phonon, etc. Similar conclusions based upon the coupled-channel calculations were also reported by Timmers *et al.* [6]. It is worth mentioning here that the possibility of the neutron transfer channel is forbidden due to the negative ground state Q values as listed in Table IV. Since the fusion dynamics of the $^{40}_{20}$Ca + $^{90}_{40}$Zr system is insensitive to coupling to the neutron

TABLE IV. Q values (MeV) for ground-state to ground-state neutron pickup channels for various Ca + Zr systems, which are taken from Ref. [59].

System	$+1n$	$+2n$	$+3n$	$+4n$	$+5n$	$+6n$
$^{40}_{20}$Ca + $^{90}_{40}$Zr	−3.61	−1.44	−5.86	−4.17	−9.65	−9.05
$^{40}_{20}$Ca + $^{94}_{40}$Zr	+0.14	+4.89	+4.19	+8.12	+3.57	+4.65
$^{40}_{20}$Ca + $^{96}_{40}$Zr	+0.51	+5.53	+5.24	+9.64	+8.42	+11.62
$^{48}_{20}$Ca + $^{90}_{40}$Zr	−6.82	−9.79	−17.73	−22.67	−31.93	−37.60
$^{48}_{20}$Ca + $^{96}_{40}$Zr	−2.71	−2.82	−6.63	−8.69	−13.87	−17.00

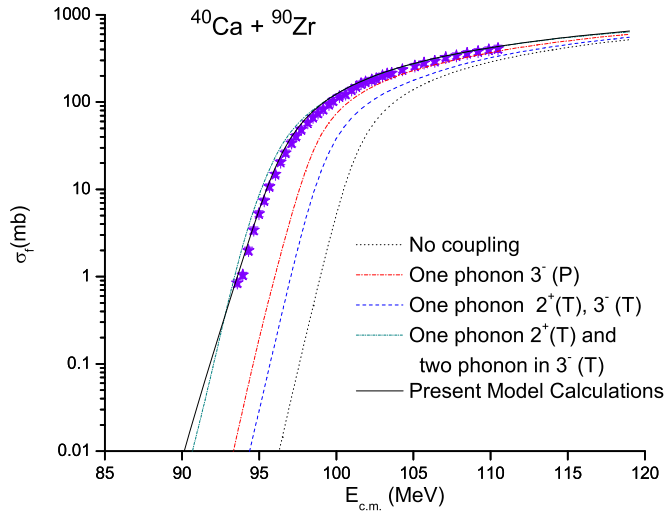

FIG. 1. (Color online) The fusion excitation function of the $^{40}_{20}$Ca + $^{90}_{40}$Zr system obtained by using the present model calculations (EDWSP model) [14–18] and the coupled-channel calculation by using the code CCFULL [55]. The results are also compared with the experimental data(*) taken from Ref. [6].

transfer channel, the relative fusion enhancement over the prediction of the one-dimensional barrier penetration model can be attributed to low-lying surface vibrational states of colliding nuclei. However, the EDWSP model in conjunction with the one-dimensional Wong's formula reproduces the experimental data in the whole range of energy. Since both the coupled-channel calculations and the present potential model calculations reasonably account for the fusion excitation function data, they reveal that the EDWSP model mocks up the effects of the inelastic surface vibrational states.

In the fusion of the $^{48}_{20}$Ca + $^{90}_{40}$Zr system, the projectile has a closed-shell structure for both proton and neutron wells, so it is more rigid as compared to the lighter projectile $^{40}_{20}$Ca, and hence it is expected to have a weak influence on the fusion dynamics. When both colliding nuclei are taken as inert, then the fusion cross section is simply influenced by the relative motion of the collision partners, and the theoretical calculations fail quantitatively to account for the experimental data. The inclusion of the single phonon 2^+ and 3^- vibrational states of both the projectile and the target along with their mutual coupling in the coupled-channel model calculations bring the prediction nearer to the data but still unable to give close agreement with the fusion data.

In the coupled-channel analysis that accounts for the experimental data in the whole range of energy, it is necessary to include the coupling to double-phonon states along their mutual couplings in the target and single phonon 2^+ and 3^- vibrational states in the projectile as shown in Fig. 2. It was found that the energy dependence of the sub-barrier fusion cross section is almost insensitive to the addition of higher multiphonon vibrational states of the target.

The success of the coupled-channel prediction for the above two systems gives an idea that coupling to the same degrees of freedom must be true for the fusion of the $^{48}_{20}$Ca + $^{96}_{40}$Zr system, wherein the target nucleus is a magic nucleus as

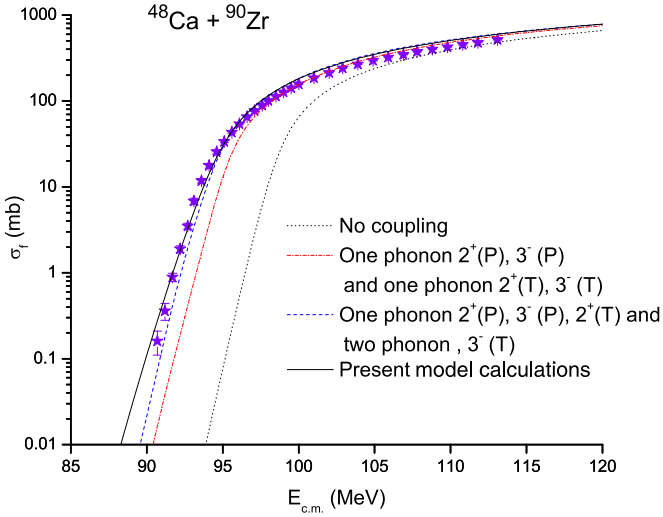

FIG. 2. (Color online) The same as Fig. 1 but for the $^{48}_{20}$Ca + $^{90}_{40}$Zr system. The experimental data (*) are taken from Ref. [56].

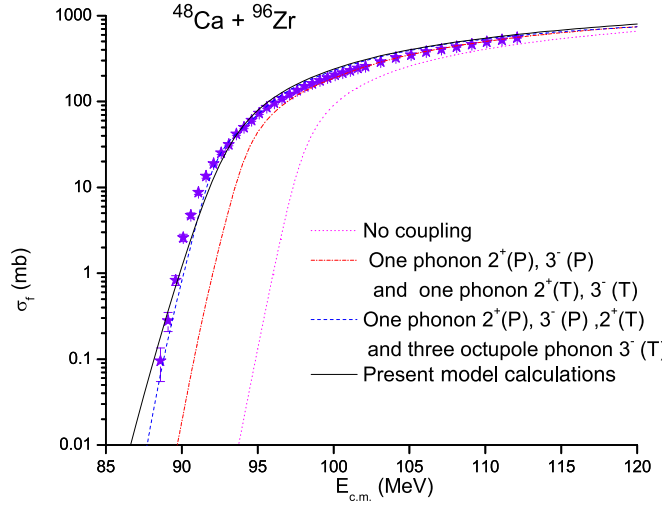

FIG. 3. (Color online) The same as Fig. 1 but for the $^{48}_{20}$Ca + $^{96}_{40}$Zr system. The experimental data (*) are taken from Ref. [56].

well as neutron rich, and the effects of the inelastic surface vibration are dominating. This particular combination of the projectile-target system is considered to extract the relevant information about the intimate link between the existence of the strong octupole vibrational state in the target and the fusion enhancement in the sub-barrier energy regions. In the no-coupling limit, the fusion cross section is significantly smaller than that of the experimental data in the below barrier energy regions. The coupled-channel calculations obtained by including couplings to the one phonon 2^+ and 3^- vibrational states of both collision partners and double-phonon states along their mutual coupling in the target are not sufficient to bring the observed enhancement. This favors consideration of the higher octupole vibrational states of the target nucleus.

The further addition of coupling to the higher phonon states, such as couplings to the three phonon 3^- vibrational states in the target along with their mutual coupling, such as the $(2^+)^3$,$(3^-)^3$, $(2^+ \otimes (3^-)^2)$, and $(3^- \otimes (2^+)^2)$ states and coupling to the one phonon 2^+ state in the projectile are required to reproduce the experimental data. However, the EDWSP model calculations compensate the effects of such a strong octupole vibrational state of the target and hence reproduce the fusion cross section in all energy regions as shown in Fig. 3. The effects of the neutron transfer channel are suppressed in the fusion dynamics of the $^{48}_{20}$Ca + $^{90,96}_{40}$Zr systems because of the unavailability of the positive Q values for the neutron transfer channel as listed in Table IV. Therefore, a similar conclusion for both $^{48}_{20}$Ca + $^{90,96}_{40}$Zr systems can be drawn that the relative enhancement in the sub-barrier fusion cross section over the predictions in which relative motion is the only degree of freedom that can be attributed to the coupling to the multiphonon vibrational states of the collision partners and such effects are simulated by the present EDWSP model calculations as evident from Figs. 2 and 3.

The comparison of the experimental data for the $^{48}_{20}$Ca + $^{90,96}_{40}$Zr systems along with their corresponding theoretical calculations performed by using the EDWSP model as shown in Fig. 4 provide the unambiguous conclusion about the existence of the strong octupole vibrational state in the $^{96}_{40}$Zr nucleus. For both systems in the above barrier energy regions, both theoretical predictions and the experimental data have no difference, which clearly identifies that the energy dependence of the fusion cross section is almost insensitive to the various channel coupling effects. However, as the energy becomes smaller than the average barrier height, the striking difference in their fusion mechanisms indicates that various channel coupling effects produce pronounced fusion enhancement in the sub-barrier energy regions. The larger enhancement of the sub-barrier fusion excitation function data for the $^{48}_{20}$Ca + $^{96}_{40}$Zr system in comparison to that of the $^{48}_{20}$Ca + $^{90}_{40}$Zr system directly mirrors the effects of the strong octupole vibrations in the heavier target $^{96}_{40}$Zr.

The keen interest in fusion of the $^{40}_{20}$Ca + $^{94,96}_{40}$Zr systems [6,56,58–63] lies in their positive ground state Q values for

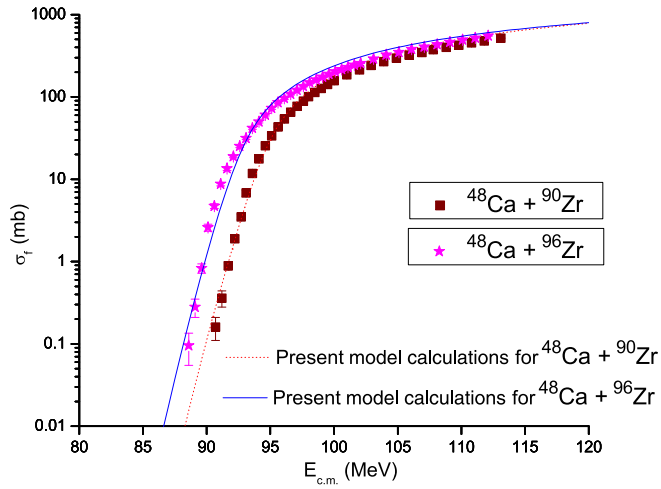

FIG. 4. (Color online) The fusion excitation function data of the $^{48}_{20}$Ca + $^{90,96}_{40}$Zr systems [56] along with the results obtained by using the present model calculations [14–18].

the neutron transfer channels, which are expected to play a decisive role in the relative enhancement of the fusion cross section in below barrier energies. In the fusion of the $^{40}_{20}$Ca + $^{94}_{40}$Zr system, the coupling to the octupole vibrations in the projectile alone leads to a significantly larger fusion cross section than that of the no-coupling case but is unable to bring the observed experimental data. The coupled-channel calculations obtained by the adding of coupling to the two and three phonon 3^- vibrational states in the target and the one phonon 3^- vibrational state of the projectile fail badly to reproduce the fusion data. The coupling to the four phonon 3^- vibrational state brings additional enhancement, but still there is a large discrepancy between the coupled-channel prediction and the experimental data. The further addition of higher multiphonon vibrational states in the target $^{94}_{40}$Zr nucleus has no effect on the energy dependence of the sub-barrier fusion cross section as shown in Fig. 5.

In the target $^{94}_{40}$Zr, there are four neutrons outside of the neutron closed shell $N = 50$, so the probability of the transfer of six neutrons from the target to the projectile is very high due to positive ground state Q values. The failure of the coupled-channel calculations to account for the experimental data for the $^{40}_{20}$Ca + $^{94}_{40}$Zr system suggests that it is fruitful to couple all the possible neutron transfer channels to reproduce the experimental data in an economical way.

To disentangle the importance of neutron transfer couplings, the present analysis also includes the fusion of the $^{40}_{20}$Ca + $^{96}_{40}$Zr system wherein the existence of the strong octupole vibrations in both colliding nuclei has been pointed out in literature. In the target, there are six neutrons outside of the neutron shell closure, which occurs at $N = 50$, and this leads to the possibilities of at least six neutron transfers from the target to the projectile with positive neutron transfer Q values as given in Table IV. The results of the coupled-channel calculations for the $^{40}_{20}$Ca + $^{96}_{40}$Zr system are found to be similar to those of the $^{40}_{20}$Ca + $^{94}_{40}$Zr system. The coupling to the one-phonon octupole surface vibration in the projectile and the couplings to the two-phonon and three-phonon octupole vibrational states in target are significantly underpredicted by

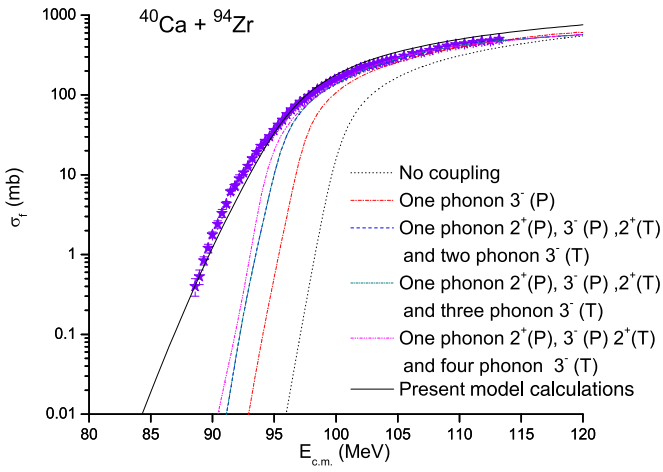

FIG. 5. (Color online) The same as Fig. 1 but for the $^{40}_{20}$Ca + $^{94}_{40}$Zr system. The experimental data (*) are taken from Ref. [59].

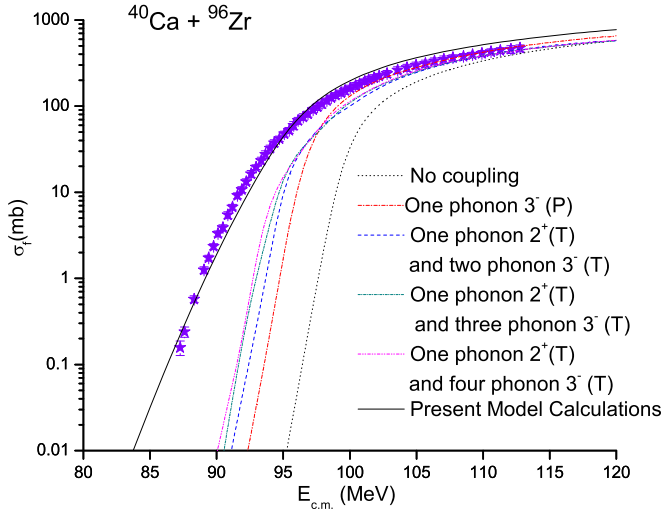

FIG. 6. (Color online) The same as Fig. 1 but for the $^{40}_{20}$Ca + $^{96}_{40}$Zr system. The experimental data (*) are taken from Ref. [6].

the experimental data. The further addition of four phonons in the target improves the results quantitatively but fails miserably to reproduce the experimental data in below barrier energy regions. The couplings to the existence of the strong octupole vibration in both colliding nuclei are expected to modify to the energy dependence of the fusion cross section in the energy regions close to the Coulomb barrier. However, the inclusion of such vibrational states fails to bring the required order of magnitude of the sub-barrier fusion excitation function data in all ranges of energy as shown in Fig. 6. The prescription of the EDWSP model works extremely well and gives quite close agreement between the theoretical prediction and the experimental data. Thus, the EDWSP model reasonably accounts for the effects of the inelastic surface vibrations of the collision partners as well as the influence of the neutron transfer channels on the fusion dynamics of the $^{40}_{20}$Ca + $^{94,96}_{40}$Zr systems as evident from Figs. 5 and 6.

The comparison of the experimental data for the $^{40}_{20}$Ca + $^{90,94,96}_{40}$Zr systems along with the present model calculations will help to extract the unambiguous picture with regard to the rich interplay of the multiphonon vibrational states of the collision partners and neutron pickup channels. Above the Coulomb barrier, the situation is quite similar for both theoretical calculations and corresponding experimental data among the three cases as already discussed in Fig. 4. However, in the sub-barrier energy regions, the striking difference between the experimental data in all three systems can be understood in terms of couplings to the multiphonon inelastic surface excitations and the nucleon transfer channels. Since the strong octupole vibration in the projectile contributes equally in all three cases, the significantly larger experimental fusion data for both $^{40}_{20}$Ca + $^{94,96}_{40}$Zr systems in comparison to that of the $^{40}_{20}$Ca + $^{90}_{40}$Zr system can be attributed to the existence of a very large probability for the neutron transfer channel with positive ground state Q values. Recently, a similar conclusion with regard to the importance of the neutron transfer channels with ground state positive Q values for these systems has been

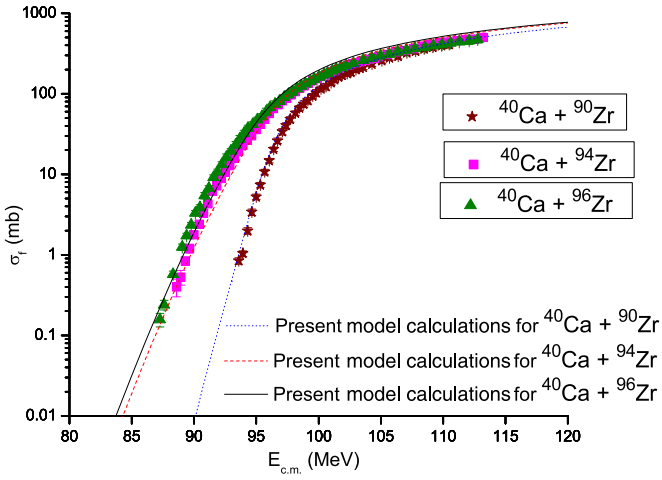

FIG. 7. (Color online) The same as Fig. 4 but for the $^{40}_{20}$Ca + $^{90,94,96}_{40}$Zr systems. The experimental data for these systems are taken from Refs. [6,59].

pointed out by several authors [64–66]. In the fusion of the $^{40}_{20}$Ca + $^{94,96}_{40}$Zr systems, the possibility of the transferring of six neutrons from the target to the projectile is very large, and the effects of the neutron transfer channels are almost same in both cases. Furthermore, the larger experimental fusion data for the $^{40}_{20}$Ca + $^{96}_{40}$Zr system in comparison to that of the $^{40}_{20}$Ca + $^{94}_{40}$Zr system can be linked with the existence of the strong octupole vibration in the $^{96}_{40}$Zr nucleus as evident from Fig. 7.

It is well known that the coupling to the internal degrees of freedom of collision partners, such as static deformation, surface inelastic channels, and neutron transfer channels, etc., leads to a distribution of barriers of varying heights. Similarly, an energy-dependent Woods-Saxon nuclear potential model, which simulates various channel coupling effects, results in a set of barriers of varying heights and hence reasonably explains the experimental data in the whole range of energy. In other words, the effective capture radius of the fusing nuclei is increased when the relative motion of the colliding nuclei is coupled to their intrinsic degrees of freedom. This suggests that the fusion process starts at much longer distances of separation between the reactants and hence leads to anomalously large enhancement of the fusion excitation function data. The similar features of the heavy-ion fusion reactions are evident from the present model calculations. This raises the questions on the inconsistency of the static Woods-Saxon potential, which is generally used for exploring the energy dependence of the sub-barrier fusion mechanisms. Therefore, the coupling to the inelastic surface vibrations and neutron transfer channel, whether they represent a true picture of the relevant channels in the enhancement of the fusion excitation function data or simply mock up the inconsistency of the energy-independent Woods-Saxon potential parameters, requires more intensive studies. Furthermore, the energy dependence of the diffuseness parameter (i.e., the energy dependence of the Woods-Saxon potential) is a true representation of the nuclear potential, or the mock up of the other dynamical effects is still not clear.

IV. CONCLUSIONS

The present paper addresses the interplay of the inelastic surface vibrations and the neutron transfer channels with a positive ground state Q value in the fusion dynamics of various heavy-ion systems. The fusion of the $^{40}_{20}$Ca + $^{90}_{40}$Zr and $^{48}_{20}$Ca + $^{90,96}_{40}$Zr systems is dominated by the couplings to the low-lying surface vibrational states, whereas the fusion of the $^{40}_{20}$Ca + $^{94,96}_{40}$Zr systems has the dominance of coupling to neutron transfer channels with positive ground state Q values. The strong octupole vibrations in both $^{40}_{20}$Ca and $^{96}_{40}$Zr nuclei produce pronounced effects in sub-barrier fusion enhancement. Both the coupled-channel model and the present energy-dependent Woods-Saxon potential model reasonably account for the experimental data for the $^{40}_{20}$Ca + $^{90}_{40}$Zr and $^{48}_{20}$Ca + $^{90,96}_{40}$Zr systems in all ranges of energies. However, the failure of the coupled-channel analysis to reproduce experimental data for the $^{40}_{20}$Ca + $^{94,96}_{40}$Zr systems suggest that coupling to the neutron transfer channels is necessarily required to reproduce the fusion data. However for these systems, the present potential model accounts for the experimental data in an economical way in the whole range of energy and mocks up the various dominating channel coupling effects. Furthermore, a wide range of values of diffuseness parameters, which range from ($a = 0.85$ to $a = 0.97$ fm), which is much larger than the value extracted from the elastic scattering data ($a = 0.65$ fm), is required to bring the observed experimental data.

[1] M. Beckerman, Rep. Prog. Phys. **51**, 1047 (1988).
[2] M. Dasgupta *et al.*, Annu. Rev. Nucl. Part. Sci. **48**, 401 (1998).
[3] A. B. Balantekin and N. Takigaw, Rev. Mod. Phys. **70**, 77 (1998).
[4] L. F. Canto, P. R. S. Gomes, R. Donangelo, and M. S. Hussein, Phys. Rep. **424**, 1 (2006).
[5] K. Hagino and N. Takigawa, Prog. Theor. Phys. **128**, 1001 (2012).
[6] H. Timmers *et al.*, Phys. Lett. B **399**, 35 (1997).
[7] J. O. Newton, R. D. Butt, M. Dasgupta, D. J. Hinde, I. I. Gontchar, C. R. Morton, and K. Hagino, Phys. Rev. C **70**, 024605 (2004).
[8] J. O. Newton *et al.*, Phys. Lett. B **586**, 219 (2004).
[9] K. Hagino and N. Rowley, Phys. Rev. C **69**, 054610 (2004).
[10] K. Hagino, T. Takehi, A. B. Balantekin, and N. Takigawa, Phys. Rev. C **71**, 044612 (2005).
[11] K. Washiyama, K. Hagino, and M. Dasgupta, Phys. Rev. C **73**, 034607 (2006).
[12] C. H. Dasso and G. Pollarolo, Phys. Rev. C **68**, 054604 (2003).
[13] A. Mukherjee, D. J. Hinde, M. Dasgupta, K. Hagino, J. O. Newton, and R. D. Butt, Phys. Rev. C **75**, 044608 (2007).
[14] M. Singh, S. S. Duhan, and R. Kharab, Mod. Phys. Lett. A **26**, 2129 (2011); Atti Della "Fondazione Giorgio Ronchi" Anno LXV **6**, 751 (2010).
[15] M. Singh *et al.*, Nucl. Phys. A **897**, 179 (2013).

[16] M. Singh *et al.*, Nucl. Phys. A **897**, 198 (2013); M. Singh, M. Phil., Dissertation, Kurukshetra University Kurukshetra, Haryana, India, 2009 (unpublished); M. Singh, Ph.D thesis, Kurukshetra University Kurukshetra, Haryana, India, 2013 (unpublished).
[17] M. Singh *et al.*, in *Analysis of Fusion Excitation Function Data of Heavy Ions Through an Energy Dependent Potential*, edited by S. Kumar and A. K. Jain, AIP Conf. Proc. No. 1524 (AIP, New York, 2013), p. 163.
[18] M. Singh *et al.*, EPJ Web Conf. **66**, 03043 (2014).
[19] A. M. Stefanini *et al.*, Nucl. Phys. A **456**, 509 (1986).
[20] D. Galetti and M. A. Candido Ribeiro, Phys. Rev. C **50**, 2136 (1994).
[21] C. L. Jiang *et al.*, Phys. Rev. Lett. **89**, 052701 (2002).
[22] C. L. Jiang *et al.*, Phys. Rev. Lett. **93**, 012701 (2004).
[23] C. L. Jiang, H. Esbensen, B. B. Back, R. V. F. Janssens, and K. E. Rehm, Phys. Rev. C **69**, 014604 (2004).
[24] C. L. Jiang, B. B. Back, H. Esbensen, R. V. F. Janssens, and K. E. Rehm, Phys. Rev. C **73**, 014613 (2006).
[25] T. Ichikawa, K. Hagino, and A. Iwamoto, Phys. Rev. C **75**, 064612 (2007).
[26] H. Esbensen and Ş. Mişicu, Phys. Rev. C **76**, 054609 (2007).
[27] T. Ichikawa, K. Hagino, and A. Iwamoto, Phys. Rev. Lett. **103**, 202701 (2009).
[28] R. A. Broglia, C. H. Dasso, S. Landowne, and A. Winther, Phys. Rev. C **27**, 2433(R) (1983).
[29] N. Rowley *et al.*, Phys. Lett. B **254**, 25 (1991).
[30] J. X. Wei *et al.*, Phys. Rev. Lett. **67**, 3368 (1991).
[31] A. M. Stefanini *et al.*, Phys. Rev. Lett. **74**, 864 (1995).
[32] G. P. A. Nobre, L. C. Chamon, L. R. Gasques, B. V. Carlson, and I. J. Thompson, Phys. Rev. C **75**, 044606 (2007).
[33] M. Trotta, A. M. Stefanini, L. Corradi, A. Gadea, F. Scarlassara, S. Beghini, and G. Montagnoli, Phys. Rev. C **65**, 011601(R) (2001).
[34] B. B. Back *et al.*, Rev. Mod. Phys. **86**, 317 (2014).
[35] J. R. Leigh *et al.*, Phys. Rev. C **52**, 3151 (1995).
[36] A. A. Sonzogni, J. D. Bierman, M. P. Kelly, J. P. Lestone, J. F. Liang, and R. Vandenbosch, Phys. Rev. C **57**, 722 (1998).
[37] A. M. Vinodkumar *et al.*, Phys. Rev. C **53**, 803 (1996).
[38] N. V. S. V. Prasad *et al.*, Nucl. Phys. A **603**, 176 (1996).
[39] T. Rumin, K. Hagino, and N. Takigawa, Phys. Rev. C **61**, 014605 (1999).
[40] V. I. Zagrebaev, Phys. Rev. C **67**, 061601 (2003).
[41] H. Q. Zhang *et al.*, Phys. Rev. C **82**, 054609 (2010).
[42] N. Rowley, Phys. Lett. B **282**, 276 (1992).
[43] O. N. Ghodsi *et al.*, Phys. Rev. C **86**, 024615 (2012).
[44] K. Hagino, N. Rowley, and M. Dasgupta, Phys. Rev. C **67**, 054603 (2003).
[45] N. Van Sen, R. Darves-Blanc, J. C. Gondrand, and F. Merchez, Phys. Rev. C **20**, 969 (1979).
[46] K. Nagatani and J. C. Peng, Phys. Rev. C **19**, 747 (1979).
[47] R. N. Sagaidak, S. P. Tretyakova, S. V. Khlebnikov, A. A. Ogloblin, N. Rowley, and W. H. Trzaska, Phys. Rev. C **76**, 034605 (2007).
[48] N. Wang and W. Scheid, Phys. Rev. C **78**, 014607 (2008).
[49] I. Dutt and R. K. Puri, Phys. Rev. C **81**, 064609 (2010).
[50] D. Jain *et al.*, Nucl. Phys. A **915**, 106 (2013).
[51] O. N. Ghodsi and R. Gharaei, Eur. Phys. J. A **48**, 21 (2012).
[52] R. Kumari, Nucl. Phys. A **917**, 87 (2013).
[53] C. K. Phookan and K. Kalita, Nucl. Phys. A **899**, 29 (2013).
[54] S. S. Duhan *et al.*, Mod. Phys. Lett. A **26**, 1017 (2011); Int. J. Mod. Phys. E **21**, 1250054 (2012); Commun. Theor. Phys. **55**, 649 (2011); Phys. At. Nucl. **74**, 49 (2011).
[55] K. Hagino, N. Rowley, and A. T. Kruppa, Comput. Phys. Commun. **123**, 143 (1999).
[56] A. M. Stefanini *et al.*, Phys. Rev. C **73**, 034606 (2006).
[57] C. Y. Wong, Phys. Rev. Lett. **31**, 766 (1973).
[58] H. Timmers *et al.*, Nucl. Phys. A **633**, 421 (1998).
[59] A. M. Stefanini *et al.*, Phys. Rev. C **76**, 014610 (2007).
[60] S. Kalkal *et al.*, Phys. Rev. C **81**, 044610 (2010).
[61] A. M. Stefanini *et al.*, Phys. Rev. C **62**, 014601 (2000).
[62] G. Pollarolo and A. Winther, Phys. Rev. C **62**, 054611 (2000).
[63] G. Montagnoli *et al.*, Eur. Phys. J. A **15**, 351 (2002).
[64] A. M. Stefanini *et al.*, Phys. Lett. B **728**, 639 (2014).
[65] H. Esbensen and A. M. Stefanini, Phys. Rev. C **89**, 044616 (2014).
[66] C. L. Jiang, K. E. Rehm, B. B. Back, H. Esbensen, R. V. F. Janssens, A. M. Stefanini, and G. Montagnoli, Phys. Rev. C **89**, 051603(R) (2014).
[67] D. L. Hill and J. A. Wheeler, Phys. Rev. **89**, 1102 (1953).
[68] L. C. Vaz and J. M. Alexander, Phys. Rev. C **10**, 464 (1974).
[69] J.-L. Dethier and F. Stancu, Phys. Rev. C **23**, 1503 (1981).
[70] H. Esbensen, S. Landowne, and C. Price, Phys. Rev. C **36**, 1216 (1987).